Appl Phys B (2012) 108:255–260
DOI 10.1007/s00340-012-4891-2

Applied Physics B
Lasers and Optics

Coupling external cavity mid-IR quantum cascade lasers with low loss hollow metallic/dielectric waveguides

P. Patimisco · V. Spagnolo · M.S. Vitiello · A. Tredicucci · G. Scamarcio · C.M. Bledt · J.A. Harrington

Received: 11 October 2011 / Revised version: 28 November 2011 / Published online: 7 February 2012

Abstract We report on the optical coupling between hollow core waveguides and external cavity mid-IR quantum cascade lasers (QCLs). Waveguides with 1000 μm bore size and lengths ranging from 2 to 14 cm, with metallic (Ag)/dielectric (AgI or polystyrene) circular cross-section internal coatings, have been employed. Our results show that the QCL mode is perfectly matched to the hybrid HE_{11} waveguide mode, demonstrating that the internal dielectric coating thickness is effective to suppress the higher losses TE-like modes. Optical losses down to 0.44 dB/m at 5.27 μm were measured in Ag/polystyrene-coated waveguide with an almost unitary coupling efficiency.

1 Introduction

Mid-infrared optical waveguides are conventionally fabricated by using low loss materials, e.g., chalcogenide glasses [1], fluoride glasses [2], single-crystal sapphire [3], polycrystalline thallium bromide and thallium bromoiodide [4], or silicon [5]. The best solid-core fibers typically show attenuation losses down to 0.14 dB/m. More recently, hollow waveguides have been identified as an interesting alternative to guide mid-IR optical beams. Cylindrical hollow waveguides exploit multiple reflections by internal walls of the hollow core, thus allowing confinement of radiation predominantly in the air region with marginal absorption inside the walls.

Extensive studies on metallic, circular cross-section hollow waveguides [6] demonstrated that to reduce the losses and enhance the reflectivity at the internal walls, high-index dielectric films can be deposited over the metallic layer, following an analogous approach used to make high-reflectance mirrors. The thickness of the dielectric film chosen for minimizing losses depends on the wavelength of the propagating light. Hollow-core metallic/dielectric waveguides have been fabricated using a vast variety of techniques and geometries. In the mid-IR region physical vapor deposition of silver and dielectric layers on metallic substrates [7], sputtering of metallic and dielectric films on a mandrel [8], liquid phase formation of coatings inside plastic [9] and glass [10] tubing have been employed.

In this work we report on experimental studies aiming at coupling hollow waveguides having a metal and/or internal dielectric coating with mid-IR quantum cascade lasers (QCLs). The mid-IR spectral range (i.e., from 3 to 14 μm) is quite appealing for a large number of security and defense related applications, since the main absorption features of the several chemical compounds of interest for such applications fall in this spectral window. Moreover, fiber optics is a key enabling technology needed to improve the compactness and effectiveness of detection and calibration systems, like quartz-enhanced photoacoustic (QEPAS) cells for trace gas sensing [11].

We demonstrate that the QCL beam can be coupled with high efficiency (>90%) and transmission losses lower than

P. Patimisco (✉) · V. Spagnolo · G. Scamarcio
CNR-IFN and Dipartimento Interateneo di Fisica, Università and Politecnico di Bari, Via Amendola 173, 70126 Bari, Italy
e-mail: pietro.patimisco@fisica.uniba.it

M.S. Vitiello
CNR—Istituto Nazionale di Fisica Applicata Nello Carrara, Via Madonna del Piano 1, 50019 Sesto Fiorentino, Italy

M.S. Vitiello · A. Tredicucci
NEST, Istituto Nanoscienze—CNR and Scuola Normale Superiore, Piazza San Silvestro 12, 56127 Pisa, Italy

C.M. Bledt · J.A. Harrington
Dept. Material Science & Engineering, Rutgers University, Piscataway, NJ 08855, USA

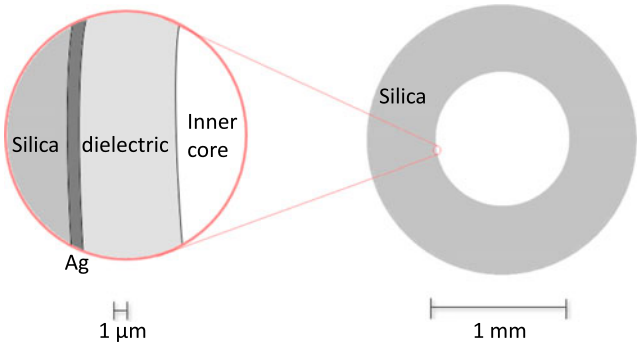

Fig. 1 Cross-section of the cylindrical hollow waveguides. The inner part consists of a metallic Ag layer coated by a single dielectric film of AgI or Polystyrene (PS) or by AgI/PS double dielectric film. The outer part consists of silica with a UV acrylate external coating

1 dB/m. The measured far-field spatial intensity distribution at the waveguide exit is determined by the dielectric coating and the launch conditions (i.e. the choice of input coupling lens to focalize the laser beam into the waveguide entrance).

2 Experimental set-up

Figure 1 shows the cross section of the employed hollow core cylindrical waveguides (HCW). HCWs are made of silica tubes with a polymer (UV acrylate) coating on the outside surface and a 1 µm thick Ag film on the internal surface, following the experimental procedure described in [12]. The Ag thickness is limited to 1 µm, since thicker films would increase surface roughness, resulting in additional loss due to scattering. However, the film thickness is larger than the Ag skin depth at mid-IR frequencies. In order to reduce the overall waveguide transmission losses due to the absorption of radiation in the metallic layer, the waveguide core is additionally coated with dielectric films using dynamic liquid phase deposition. Actually the losses at IR wavelengths are greatly reduced by adding dielectric thin films as opposed to simply using Ag coated guides. This is due to the reflection enhancement resulting from the addition of dielectric films such as AgI and PS due to thin film interference effects. CO_2 laser attenuation measurements at $\lambda = 10.6$ um have shown at least a tenfold reduction in the loss of AgI dielectric coated hollow glass waveguides over their Ag only coated counterparts [13]. HCWs having lengths in the range 2–14 cm and bore diameters of 1 mm have been used to guide the optical beam of external cavity edge emitting mid-IR QCLs. Three different coating configurations were tested: (i) AgI (0.6 µm); (ii) Polystyrene (PS) (7.7 µm); (iii) AgI/PS (0.6/7.7 µm). In all cases the coating is expected to reduce the mode dispersion and the attenuation of the lower losses optical modes. Indeed adding a thin film on the inner surface of the metallic wall changes the boundary conditions and can in principle reverse the dominant mode order. The thickness d for a non-absorbing coating can be optimized to enhance or suppress specific modes. Specifically the inner coating thickness should be larger than the critical value,

$$d_{ps} = \frac{\pi}{4k}\frac{1}{\sqrt{n^2-1}} \tag{1}$$

where k is the wave vector and n is the dielectric refractive index [14]. In the case of AgI coatings we can tailor the dielectric film thickness d_{AgI} for the desired wavelength of the application, which corresponds to the related maximal loss reduction, by using the following equation [15]:

$$d_{\mathrm{AgI}} = \frac{\lambda_0}{2\pi\sqrt{n_{\mathrm{AgI}}^2-1}}\tan^{-1}\left[\frac{n_{\mathrm{AgI}}}{(n_{\mathrm{AgI}}^2-1)^{1/4}}\right] \tag{2}$$

where λ_0 is the target wavelength and n_{AgI} is the dielectric film material refractive index. A Sn^{2+} pre-treatment is used for depositing the initial Ag film on the silica. Ag deposition has been carried out at a volumetric flow rate of 5.0 mL/min. The AgI film is deposited directly on the Ag layer at a flow rate of 11.5 mL/min, in order to have a coating thickness approximately equal to the critical one. The Ag/PS waveguides have been realized by dissolving the polystyrene in toluene at a concentration of 25 wt% and by coating the waveguide sample at a flow rate of about 0.25 mL/min. Thin film thickness of dielectric layers in hollow waveguides can be calculated through the analysis of interference absorption peaks in the infrared spectrum. A generalization of the equation to determine the thickness of dielectric thin films in a waveguide from the distance in wavenumber of adjacent interference peaks of arbitrary order is [16]:

$$d = \frac{(k_a - k_{a-1})}{4\cdot\sqrt{n^2-1}} \tag{3}$$

where d is the dielectric layer thickness, a is an integer defining the order of the chosen peak studied, k_a is the centroid wavenumber of the ath order peak, k_{a-1} is the centroid wavenumber of the $a-1$th order peak, and n is the refractive index of the material.

In the present experiments the inner coating thickness has been estimated by employing a Thermo Nicolet Protégé 460 FTIR Spectrometer equipped with a InSb detector. Taking into account the average peak spacing and the index of refraction of either polystyrene $n = 1.58$ or AgI film (2.14) a PS film thickness of about 7 µm, and a AgI thickness of 0.6 µm have been estimated. Two commercial QCL sources based on an external cavity (EC) configuration were used. Standard DFB QCLs are characterized by a larger beam divergence with respect to external cavity QCLs; thus we select these kinds of sources since better coupling results are expected, particularly in the back-to-back configuration. The chosen emission wavelengths, falling in the related mode-hop free regions, are $\lambda_a = 5.27$ µm (Daylight Solutions Inc.

model #21052-MHF, λ_a-QCL) and $\lambda_b = 10.5$ μm (Daylight Solutions Inc. model #21106-MHF, λ_b-QCL). Both lasers were driven by applying a sinusoidal dither to the diode laser current at a frequency of 16 kHz. The QCLs current were set at 360 mA (λ_a) and 900 mA (λ_b). The average optical powers measured using a pyroelectric detector were 93 mW (λ_a) and 65 mW (λ_b), respectively. At the employed laser wavelengths the critical coating thicknesses of the PS film are $d_{PS} = 0.53$ um (λ_a-QCL) and $d_{PS} = 1.1$ um (λ_b-QCL). The latter values are well below the dielectric film thickness deposited in the inner waveguide core. For the Ag/AgI waveguides $d_{AgI} = 0.45$ μm (λ_a-QCL) or $d_{AgI} = 0.9$ μm (λ_b-QCL), i.e. slightly below and well above the employed value, respectively. Considering the measured d_{AgI} film thickness we expected lower losses for a λ_a-QCL.

The coupling between the QCL and the hollow waveguide was achieved by using two different experimental approaches [17], schematically represented in Figs. 2a and 2b. In the first approach, a ZnSe lens was used to focus the collimated laser beam into a roughly 100 μm spot at the waveguide entrance. The use of a focusing lens is necessary to have an input spot size smaller than the waveguide bore diameter, in order to reduce the amount of energy blocked by the waveguide wall. Moreover, a smaller f-number launch reduces the heating due to light absorption from waveguide walls, which is a critical point for high-power applications. To record the mode profile at about 2 cm away from the waveguide output, a pyroelectric detector with a sensitive area of 1 mm × 1 mm was mounted above a compact motorized XY stage. The 2-D multi-point image of the beam profile was obtained by recording the total transmitted power 2 cm away from the waveguide output in the far field for each scanning position with a spatial resolution of about 0.2 μm for both scanning directions. The second approach, called back-to-back configuration, was obtained by placing the hollow waveguide at about 4 mm from the QCL (Fig. 2b). A steel circular pinhole with the same diameter of the hollow core was placed in contact with the waveguide to prevent detection of scattered light not propagating through the waveguide.

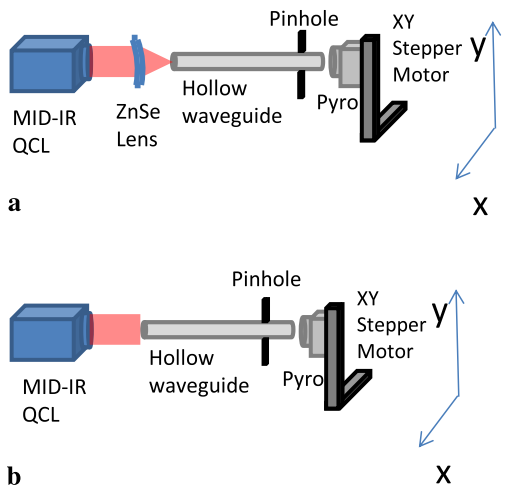

Fig. 2 Schematics of the experimental setup. The laser beam is focused at the waveguide entrance using a ZnSe lens (**a**) or in a simple back-to-back configuration (**b**) and detected using a pyroelectric detector (Pyro)

3 Results and discussion

Figures 3a–b shows the far-field spatial intensity distribution of the two employed QCL sources measured while shining the unfocused beams on the detector sensitive area. The beam profile of the laser emitting at 5.27 μm is divergent and asymmetric (see Fig. 3a) mostly due to a not-perfect optical coupling between the laser chip and the internal collimator lens. On the contrary the intensity distribution profile of the laser emitting at 10.5 μm is more symmetric and exhibits a Gaussian-like beam shape, as expected for a standard edge emitting QCL.

Figures 4a–f show the far-field spatial intensity distribution of λ_a-QCL at the exit of a 12 cm long hollow waveguide having a AgI/PS double dielectric internal coating (a, d) or a 14 cm long waveguide having a single dielectric film of AgI (b, e) or PS (c, f). In a first experimental run (Figs. 4a–c) the QCL beam is coupled into the waveguide with a f/1 ZnSe lens that focuses the beam directly at the center of hollow waveguide, in straight condition (see Fig. 2a). In a second experimental run (Figs. 4d–f) the QCLs were placed directly

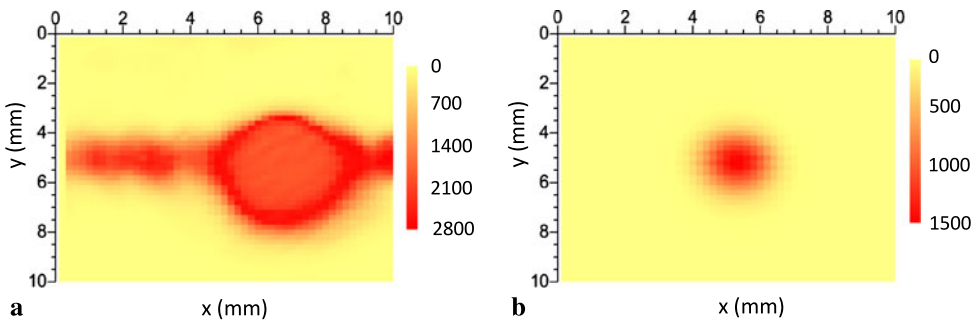

Fig. 3 Far-field spatial intensity distribution of the λ_a-QCL (**a**) and λ_b-QCL (**b**). The beam profile has been measured under the experimental configuration of Fig. 2b, but without any hollow fiber between the laser and the detector stage

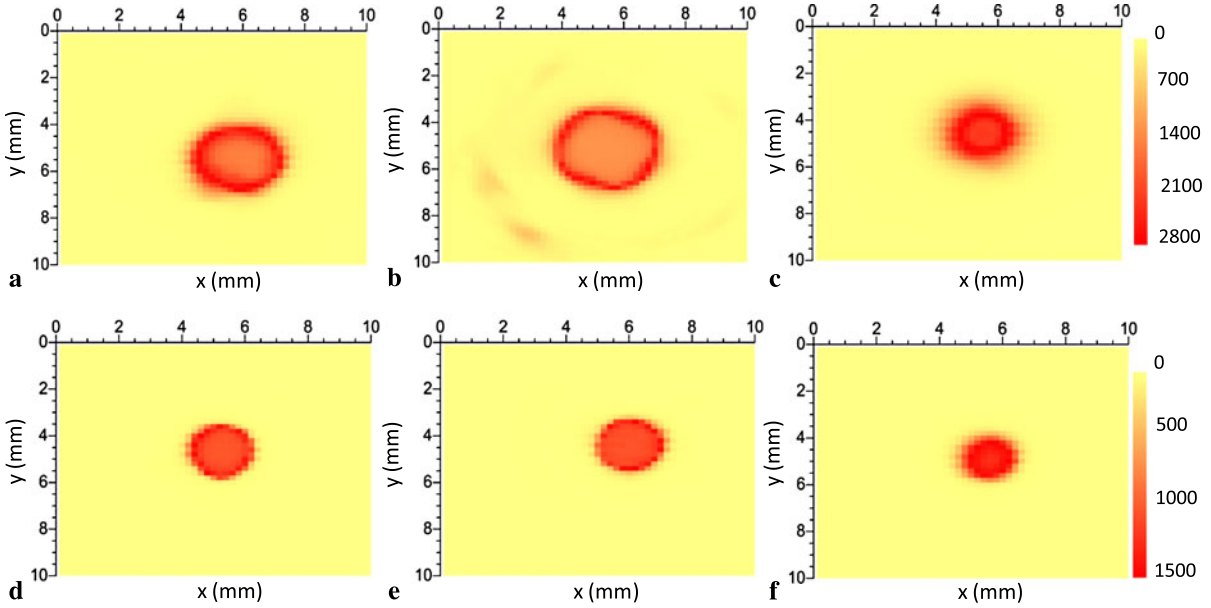

Fig. 4 Far-field spatial intensity distribution of the λ_a-QCL upon exiting a 12 cm long and 1 mm bore diameter hollow waveguide having a AgI/PS double dielectric film ((**a**), (**d**)) and a 14 cm long and 1 mm bore diameter, having a single dielectric film of AgI ((**b**), (**e**)) or a single dielectric film of PS ((**c**), (**f**)). The beam profiles have been measured by focusing the QCL beam directly at the center of the hollow waveguide by using a ZnSe lens (**a**)–(**c**), or in a back-to-back configuration (**d**)–(**f**)

in close contact with the source with no intermediate optics, in a back-to-back configuration (see Fig. 2b) [17]. The results of similar experiments performed for the λ_b-QCL are shown in Figs. 5a–f. The electric field intensity distribution shows that the QCL mode is perfectly matched to the hybrid HE_{11} mode, for which the electric field at the boundary is reduced along the entire contour of the waveguide wall, meaning that the deposited inner dielectric coating thickness is effective to suppress the higher losses TE-like modes. The observation of a single mode profile may be surprising since, as $a \gg \lambda$, one can expected that hollow waveguides should be overmoded. However, it must be considered that in hollow waveguides the losses for the higher order modes increase as the mode parameter squared. Thus the loss for the higher-order modes becomes so high that they are damped out and only the lowest-order modes can propagate [13]. Thus, our results demonstrate that the HE_{11} mode loss in an optimally designed waveguide can become lower than the TE_{01} mode loss [18], even for dielectric coatings with a moderate absorption coefficient. The small interference fringes visible in the beam profile of Fig. 3a are no more visible in Fig. 4, thus demonstrating that the use of a hollow core waveguide is beneficial in terms of beam profile cleaning, leading to a laser beam symmetric output.

For what concerns the far-field spatial intensity distribution of the laser at 10.5 μm, the results of Fig. 5 clearly show that the beam maintains a Gaussian shape after propagation through the waveguide while maintaining a perfect match with the HE_{11} optical mode. It is worth noticing that the output beam profile of hollow waveguides depends not only on the bore diameter but also on the quality and launch conditions (with or without focal lens) of the input laser. In particular, the output beam divergence of these waveguides depends mostly on three factors: (i) the nature of the optical mode propagating through the guide; (ii) the wavelength and the polarization of the incoming beam; (iii) the bore diameter. In principle the output beam divergence can give an indication of the number of modes propagating in the waveguide. We found that the beam divergence is larger when the ZnSe lens is used to focalize the laser beam at the waveguide entrance, especially for the λ_a-QCL, because additional optical modes are developed through the straight waveguide. This is particularly evident in Fig. 4b where a weak ring is developed around the main propagating mode. No changes in the propagation losses and power coupling efficiency have been observed in the mode-hop free spectral ranges for both QCLs. Absolute values of the losses of the excited mode for the straight waveguides were determined by measuring the input/output optical power at the waveguide entrance/exit by means of the following equation:

$$dB = 10\log_{10}\left(\frac{I_0}{I_s}\right) \tag{4}$$

where I_0 (I_s) is the optical power at the waveguide entrance (exit). The graph in Fig. 6 displays the values measured by coupling 2–14 cm long hollow waveguides with the λ_a-QCL under the experimental conditions schematically shown in Fig. 2b.

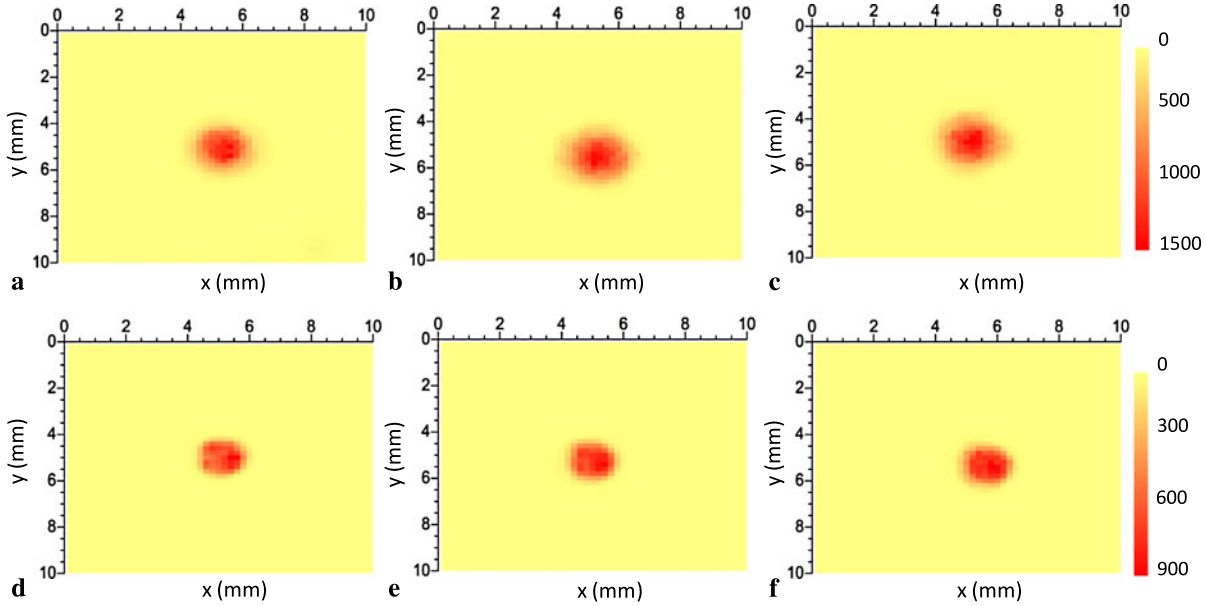

Fig. 5 Far-field spatial intensity distribution of the λ_b-QCL upon exiting a 12 cm long and 1 mm bore diameter hollow waveguide having a AgI/PS double dielectric film ((**a**), (**d**)) and a 14 cm long and 1 mm bore diameter, having a single dielectric film of AgI ((**b**), (**e**)) or a single dielectric film of PS ((**c**), (**f**)). The beam profiles have been measured by focusing the QCL beam directly at the center of the hollow waveguide by using a ZnSe lens (**a**)–(**c**), or in a back-to-back configuration (**d**)–(**f**)

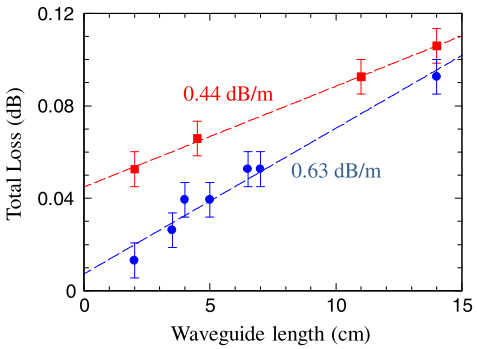

Fig. 6 Total losses calculated from the ratio of input/output power values for λ_a-QCL at the waveguide entrance/exit for Ag/AgI coatings (● symbols) and for Ag/PS coatings (■ symbols) under the experimental condition of Fig. 2a, while coupling the QCL mode preferentially with the HE_{11} waveguide mode. *The dashed lines* are linear fits to the data. The reported transmission losses have been estimated from the slope of each linear fit

The transmission losses increase linearly with the waveguide length. The linear fit to the data allows one to estimate transmission losses of 0.63 dB/m for Ag/AgI coatings and 0.44 dB/m for Ag/PS coatings. The coupling efficiency values between the QCL source and the waveguide is extracted from the intercept of the linear fits to the data. We obtained efficiency values as high as 99.8% for the AgI single dielectric film waveguide and 99.0% for Ag/PS coatings.

Unlike solid-core fibers, losses in hollow waveguides is highly dependent on the launch conditions and in particular the laser spot size (ω) and bore diameter (d) [19]. When a Gaussian beam is focused into a hollow waveguide along its axis, only the HE_{1m} modes are excited. The power coupling efficiency of the incident beam to each HE_{1m} waveguide mode depends critically on the beam waist to bore radius ratio ω/d. At small f-numbers more power is coupled to the higher-order modes and at larger f-numbers the beam can be clipped by waveguide walls. Since the HE_{11} mode has the lowest theoretical loss, it is necessary to optimize the launching conditions to couple most of the input beam to this mode. By playing on the lens position with respect to waveguide entrance (ω/d parameter) and maximizing the output power at the waveguide exit we were able to couple most of the input beam to the lowest-loss mode, HE_{11}. Theoretically up to 98.1% of power coupling efficiency of an incident Gaussian beam to the lowest-loss HE_{11} mode can be obtained [19].

4 Conclusions

In summary, optical coupling between MIR QCLs and hollow waveguides with a single or double internal dielectric film was investigated by MIR far-field imaging. The output beam profile is always symmetric, even when the input laser beam profile is partially asymmetric (in our case, small interference fringes). The optical losses measured for 1000 μm bore diameter at 5.27 μm was 0.63 dB/m for Ag/AgI coatings and 0.44 dB/m for Ag/PS coatings, which makes it possible to use these fibers in several applications such as radiometry or chemical sensing. Preliminary results using a

single mode hollow fiber coupling system between a QCL source and a quartz-enhanced photoacoustic cell show that ∼99% of power coming out from the fiber collimator goes through the tuning fork and the micro-resonator tubes composing the QEPAS cell.

References

1. M. Anne, J. Keirsse, V. Nazabal, K. Hyodo, S. Inoue, C. Boussard-Pledel, H. Lhermite, J. Charrier, K. Yanakata, O. Loreal, J. Le Person, F. Colas, C. Compere, B. Bureau, Sensors **9**, 7398 (2009)
2. C. Kao, G.A. Hockham, Proc. IEEE **133**, 1151 (1966)
3. R. Nubling, J.A. Harrington, Appl. Opt. **36**, 5934 (1997)
4. D.A. Pinnow, A.L. Gentile, A.G. Standlee, A.J. Timpler, L.M. Hobrock, Appl. Phys. Lett. **33**, 28 (1978)
5. A. Spott, Y. Liu, T. Baehr-Jones, R. Ilic, M. Hochberg, Appl. Phys. Lett. **97**, 213501 (2010)
6. Y. Matsuura, M. Miyagi, Appl. Opt. **32**, 6598 (1993)
7. K.D. Laakmann, M.B. Levy, U.S. Patent No. 5005944 (Issued 1991)
8. M. Miyagi, A. Hongo, Y. Aizawa, S. Kawakami, Appl. Phys. Lett. **43**, 430 (1983)
9. N. Croitoru, J. Dror, I. Gannot, Appl. Opt. **29**, 1805 (1990)
10. T. Abel, J. Hirsch, J.A. Harrington, Opt. Lett. **19**, 1034 (1994)
11. V. Spagnolo, A.A. Kosterev, L. Dong, R. Lewicki, F.K. Tittel, Appl. Phys. B **100**, 125 (2010)
12. Y. Matsuura, Y. Abel, J. Hirsch, J.A. Harrington, Electron. Lett. **30**, 1688 (1995)
13. J.A. Harrington, *Infrared Fibers and Their Applications* (SPIE, Bellingham, 2004)
14. C. Dragone, IEEE Trans. Microw. Theory Tech. **28**, 704 (1980)
15. R. George, J.A. Harrington, Appl. Opt. **44**, 6449 (2005)
16. B. Bowden, J.A. Harrington, O. Mitrofanov, Opt. Lett. **32**, 2945 (2007)
17. M.S. Vitiello, J.-H. Xu, M. Kumar, F. Beltram, A. Tredicucci, O. Mitrofanov, H.E. Beere, D.A. Ritchie, Opt. Express **19**, 1122 (2011)
18. B. Bowden, J.A. Harrington, O. Mitrofanov, Appl. Phys. Lett. **43**, 181104 (2008)
19. R. Nubling, J.A. Harrington, Opt. Eng. **37**, 2452 (1998)